Journal of Materials Chemistry

Cite this: J. Mater. Chem., 2011, 21, 4450

www.rsc.org/materials

PAPER

Employing an amphiphilic interfacial modifier to enhance the performance of a poly(3-hexyl thiophene)/TiO_2 hybrid solar cell†

Yu-Ching Huang,‡[a] Jui-Hung Hsu,‡[a] Yu-Chia Liao,[a] Wei-Che Yen,[b] Shao-Sian Li,[a] Shiang-Tai Lin,[c] Chun-Wei Chen[a] and Wei-Fang Su*[ab]

Received 23rd October 2010, Accepted 22nd December 2010
DOI: 10.1039/c0jm03615c

We have studied two amphiphilic interfacial modifiers: low cost Cu phthalocyanine dye containing ether side chains (Cu–ph–ether dye) and a carboxylic acid- and bromine-terminated 3-hexyl thiophene oligomer (oligo-3HT-(Br)COOH, $M_w \sim 5K$) to enhance the interfacial interaction between poly(3-hexyl thiophene) (P3HT) and TiO_2 nanorods. A large improvement in the performance of fabricated solar cells was observed using these relatively large molecular modifiers when compared to pyridine-modified TiO_2 nanorods. UV-vis spectroscopy and X-ray photoelectron spectroscopy analyses reveal that the modifiers are adsorbed and chemically bonded to TiO_2 through unshared electrons associated with the modifiers. Furthermore, the new modifiers increased the hydrophobicity of TiO_2 with the order of oligo-3HT-(Br)COOH > Cu–ph–ether dye > pyridine. Synchrotron X-ray spectroscopy studies of the modified hybrid films indicate the crystallinity of P3HT is increased, following the same trend as the hydrophobicity, because the new modifiers function as plasticizers, increasing the flow characteristics of the film. Moreover, the same trend is also observed for the reduced recombination rate and increased lifetime of charge carriers in the device by transient photo-voltage measurement. Thus, the oligo-3HT-(Br)COOH outperforms the Cu–ph–ether dye and pyridine in enhancing the power conversion efficiency (PCE, η) of the solar cell. More than a two-fold improvement is shown compared to pyridine. The results are due to the large size, conductivity, and polar characteristics of the oligo-3HT-(Br)COOH unit, which facilitates both the crystallization of P3HT and the electron transport of the TiO_2 nanorods. This study provides a useful route for increasing the efficiency of hybrid solar cells *via* the enhancement of interfacial interactions between organic donors and inorganic acceptor materials.

Introduction

Solar cells made from hybrids of polymers and nanoparticles have attracted extensive interest due to their low weight and cost, and non-vacuum processing by reel-to-reel or spray deposition on flexible substrates. The use of inorganic nanoparticles, such as CdSe,[1,2] PbS,[3] ZnO,[4] and TiO_2,[5–8] has been explored because of their high electron mobility as well as physical and chemical stability. The use of environmentally friendly materials of low toxicity is mandatory for the development of new energy technology; therefore, we chose to utilize TiO_2 nanorods instead of CdSe or PbS nanoparticles. In addition, TiO_2 is a low cost material, which uses a low energy consumption sol–gel process in its synthesis. The working principle of a hybrid solar cell is based on the bulk heterojunction (BHJ) model;[9] the conducting polymer acts as an electron donor, harvesting sunlight, and the inorganic nanoparticles function as an electron acceptor, allowing electron transport. In BHJ structures, the excitons will diffuse to the interface between the donor and acceptor and then separate into holes and electrons. Holes and electrons should be transported efficiently to their corresponding electrodes before charge recombination; otherwise the generated photocurrent would be low. Therefore, interfacial behavior is a critical performance factor for hybrid solar cells.

Surface modification is an effective way to change the performance of materials. Researchers have found that the polymers' mobility can be improved *via* interface modification.[10,11] Recently, many researchers have reported utilizing surface modifications in photovoltaic devices to improve light harvesting,[12] enhance charge transport,[13,14] and alter film morphology.[15,16] One of the many advantages of TiO_2 is that its surface can be easily modified by organic molecules.[8,17–21] Using surface modification, the chemical and physical properties of TiO_2 can be tuned to become compatible with organic materials and generate larger interfaces. For that reason, appropriate

[a]*Department of Materials Science and Engineering, National Taiwan University, Taipei, 106-17, Taiwan. E-mail: suwf@ntu.edu.tw*
[b]*Institute of Polymer Science and Engineering, National Taiwan University, Taipei, 106-17, Taiwan*
[c]*Department of Chemical Engineering, National Taiwan University, Taipei, 106-17, Taiwan*

† Electronic supplementary information (ESI) available: molecular modelling data. See DOI: 10.1039/c0jm03615c

‡ These authors contributed equally to this work.

surface modifiers are required for a hybrid system consisting of organic and inorganic materials. These modifiers have to possess the following characteristics: to be easily anchored to the nanoparticles surface for good compatibility and capable of forming a cascade bandgap to enhance charge transport.

Up to now, Chen and co-workers[8] have found that a Ru-based dye such as N3 is a very effective surface modifier for TiO_2 that enhances the power conversion of a P3HT–TiO_2 nanorod hybrid solar cell. However, the N3 dye made from the rare metal Ru is very expensive. Ramakrishna and co-workers[21] reported high-efficiency nanoporous TiO_2–polythiophene hybrid solar cells using a metal-free organic dye, D102. The photoactive layer of this type of hybrid solar cell needs a multi-step fabrication process including (1) high temperature sintering (450 °C) of the screen printed TiO_2 nanoparticle paste on to a FTO glass substrate to obtain the nanoporous TiO_2 electrode, (2) surface modification of nanoporous TiO_2 by dye, Li salt and 4-tert-butylpyridine (TBP) and (3) spin coating P3HT on the dye-coated nanoporous TiO_2 electrode. Whereas, the photoactive layer of the P3HT–TiO_2 nanorod hybrid solar cell is prepared by simple spin coating of a mixture of P3HT with modifier-coated TiO_2 nanorods on a ITO glass substrate. The TiO_2 nanorods are prepared at a relatively low temperature of 98 °C.

In this study, we propose two new low cost surface modifiers, Cu phthalocyanine dye containing ether side chains (Cu–ph–ether dye) and oligo-3HT-(Br)COOH, to modify the surface of the TiO_2 nanorods (Fig. 1). The low cost Cu–ph–ether dye is commercially available and is an organic molecular semiconductor. It has been extensively used in compact disk manufacturing and employed as a hole-transporting material in organic devices.[22,23] The polar oligo-3HT-(Br)COOH, synthesized in our lab, is a conducting molecule. Surface characterizations were carried out to probe the interfacial interactions and to assess their impact on the performance of the P3HT–TiO_2 hybrid solar cell.

Experimental details

The high aspect ratio anatase TiO_2 nanorods were synthesized by hydrolyzing titanium tetraisopropoxide according to our previously study.[6] Oleic acid (OA, 120 g) was vigorously stirred at 120 °C for one hour in a three-neck flask under Ar flow to remove moisture. The reactant was then cooled to 98 °C and titanium tetraisopropoxide (17 mmol, Aldrich, 99.999%), as the precursor, was added into the flask and stirred for 5 min to mix with the oleic acid. Trimethylamine-*N*-oxide dihydrate (34 mmol, Acros, 98%) in 17 ml of water was rapidly injected into the flask to catalyze the polycondensation reaction. This reaction was continued for 9 h to complete the hydrolysis and crystallization. Subsequently, the TiO_2 nanorods were obtained. The TiO_2 nanorods were purified through several cycles of washing and precipitation using methanol to remove any unreacted oleic acid or impurities.

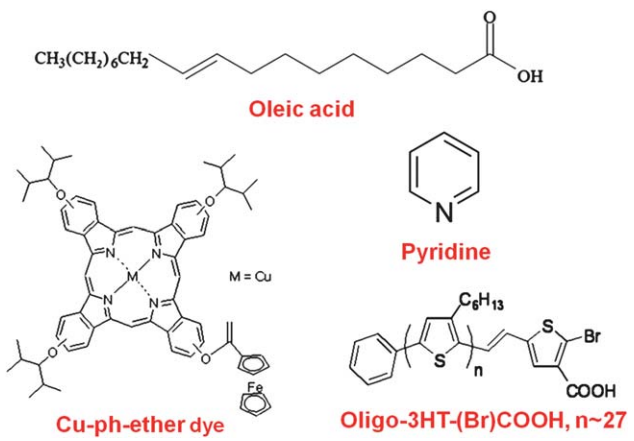

Fig. 1 The chemical structures of surface molecules involved in the surface modification process.

The oligo-3HT-(Br)COOH was synthesized through a Heck reaction using a vinyl-terminated 3-hexylthiophene oligomer and 1,4-dibromo-3-carboxylic thiophene. The α-vinyl-ω-phenyl functional ends of poly(3-hexyl thiophene) (compound 1) and 2, 5-dibromo thiophene-3-carboxylic acid (compound 2) were first synthesized by following the procedures found in the literature.[24,25] In a dry box, we combined compound 2 (0.15 g, 0.70 mmol) and compound 1 ($M_n = 7000$, 1.00 g, 0.14 mmol) in a glass reaction tube equipped with a stir bar. We then added $Pd_2(dba)_3$ (160 mg), tri(*t*-butyl)phosphine (0.15 mL), methyldicyclohexylamine (10 mL), and anhydrous THF (100 mL) into the mixture. The tube was sealed and removed from the dry box. The mixture was stirred at 55 °C for 24 h, and then cooled to room temperature. Finally, the solution was precipitated with methanol (500 mL) to give purplish polymer whiskers and further washed with methanol in a Soxhlet apparatus. The purified oligomer was dried under vacuum overnight and collected as a dark purple material.

For surface modification, the TiO_2 nanorods, end-capped with oleic acid (20 mL), were washed and precipitated by methanol (20 mL) 3 to 5 times to remove oleic acid molecules that were not tightly bound to the surface. Then pyridine (20 mL) was added to uniformly mix with the end-capped TiO_2 nanorods with the aid of an ultrasonic homogenizer. The mixture was then put into a three-neck flask and refluxed at 70 °C for 24 h under N_2 flow to obtain a transparent solution. Oleic acid molecules on the surface of the TiO_2 could be further removed in this step. Subsequently, adequate amounts of surface modifiers (Fig. 1) were dissolved into the TiO_2 solution. The Cu–ph–ether dye was obtained from SunQ Corporation of Taiwan. The solution was then heated to 70 °C and stirred for 24 h to allow the complete adsorption of surface modifiers onto the surface of TiO_2. Finally, we used an excess of hexane to precipitate the modified TiO_2 nanorods and to wash out the non-adsorbed surface modifiers.

We monitored the adsorption behavior of surface modifiers on TiO_2 nanorods by UV-visible absorption spectroscopy (PerkinElmer Lambda 35). The film thickness was determined by an α-stepper (DEKTAK 6M 24383). The surface chemistry of the TiO_2 nanorods modified with surface ligand was studied by high resolution X-ray photoelectron spectroscopy (XPS, PHI5000 Versaprobe). The dispersion of modified TiO_2 nanorods was analyzed using a JOEL JEM-1230 transmission electron microscope (TEM) operating at 120 keV. The surface hydrophobicity variation of the TiO_2 nanorods after surface modification was evaluated by a contact angle goniometer (First Ten Angstron FTA-125) using drop-cast TiO_2 nanorods samples on a glass substrate and de-ionized water as the testing liquid. The synchrotron X-ray spectroscopy was done on beam line 13A1 of

the National Synchrotron Radiation Research Center (NSRRC) in Taiwan. The HOMO and LUMO level of P3HT–TiO_2 nanorods with Cu–ph–ether dye and oligo-3HT-(Br)COOH were determined by cyclic voltammetry (CV) measurements using an electrochemical work station (CHI600B).

For the solar cell study, the hybrid material was prepared by blending the modified TiO_2 nanorods with P3HT in 53 : 47 wt/wt ratios. P3HT was dissolved in chlorobenzene and TiO_2 nanorods were dissolved in a co-solvent of pyridine, dichloromethane and chloroform in a volumetric ratio of 1 : 2 : 2. A thin active hybrid layer of P3HT–TiO_2 nanorods ~120 nm thick was spin coated onto ITO glass that was covered with about 40 nm poly(3,4-ethylenedioxythiophene)–poly(styrenesulfonate) (PEDOT:PSS) (Baytron P, 4083). The PEDOT:PSS layer was spin coated onto ITO glass and baked at 120 °C for 30 min. An additional layer of TiO_2 nanorods was deposited between the hybrid material and the Al electrode to act as a hole blocking layer. The Al electrode was then deposited onto the TiO_2 nanorod layer by thermal evaporation under vacuum at 3×10^{-6} torr.

We also measured the charge carrier lifetime and the recombination rate constant of the solar cell devices by transient photovoltage measurement. A small perturbation generated by a frequency-doubled Nd:YAG pulse laser ($\lambda = 532$ nm, repetition rate 10 Hz, duration ~5 ns) was used to generate extra electrons and holes in the hybrid films. The transient decay signals were recorded by a digital oscilloscope (Tetronix TDS5052B).

All theoretical calculations in this study are carried out using the quantum mechanical package Gaussian 03.[26] Equilibrium structures are determined using density functional theory (DFT) with the B3LYP[27,28] functional and the 6-31 + G* (oleic acid and pyridine) or 6-31G* (oligo-3HT-(Br)COOH) basis set. Properties including dipole moment are obtained from additional single point energy calculations performed at the B3LYP/6-31 + G* level. The volume and surface area are determined from the Connolly[29] molecular surface using the van der Waals atomic radii. The methyl groups are used in replacement of the hexyl side chains of oligo-3HT-(Br)COOH. A previous study[30] has shown that such simplification does not much change the calculated electronic properties, and could significantly reduce the computational time. The properties of oligo-3HT-(Br)COOH are linearly extrapolated from those of oligo*X*-3HT-(Br)COOH with $X = 3$, 5, 7, 11, and 15.

Results and discussion

We studied the adsorption behaviors of Cu–ph–ether dye and oligo-3HT-(Br)COOH on a TiO_2 surface using oligo-3HT (M_w = 8K) as a reference point. Fig. 2(a) shows the UV-vis absorption spectra of TiO_2–(oligo-3HT). The maximum peak of 450 nm is from the conjugated thiophene molecule. The peak decreased after the sample was washed with a good solvent, specifically hexane. The peak disappeared after the second washing. Thus, the oligo-3HT was loosely bonded to the TiO_2 surface *via* van der Waals forces, and can be easily removed by solvent washing. Fig. 2(b) illustrates the UV-vis absorption spectra of TiO_2–(oligo-3HT-(Br)COOH) at 1.93×10^{-1} mmol of the S atom. The maximum peak of 430 nm decreases after hexane washing. However, it does not decrease further with additional washing after the first wash. The results indicate that the oligo-

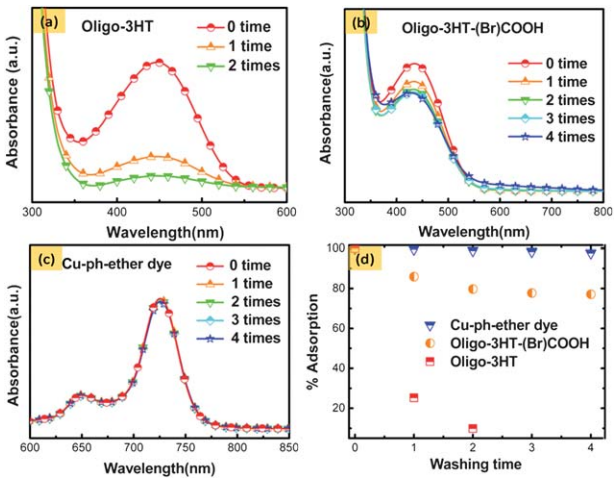

Fig. 2 Normalized UV-vis absorption spectra of (a) TiO_2–oligo-3HT, (b) TiO_2–(oligo-3HT-(Br)COOH) and (c) TiO_2–(Cu–ph–ether dye) after repeated washing steps. (d) The remaining amount of surface modifiers on TiO_2 after repeated washing steps.

3HT-(Br)COOH can adhere well to the TiO_2 surface through the chelating bond between –COOH and Ti atoms.[12] Some of the oligo-3HT-(Br)COOH was adsorbed on TiO_2 *via* the oligo-3HT segment, which can be easily removed by washing. It is very interesting to note that the Cu–ph–ether dye can adhere extremely well, as shown in Fig. 2(c). At 2.84×10^{-3} mmol of the Cu atom concentration, the maximum peak of 725 nm is clear and does not fade away with repeated hexane washing. The results indicate the Cu–ph–ether dye is likely bonded to the TiO_2 surface through the oxygen atom (ether side chain) of the Cu–ph–ether dye. The adsorption behaviors of these three surface modifiers are illustrated in Fig. 2(d). A 97% adsorption is achieved for Cu–ph–ether dye while 80% adsorption is obtained for oligo-3HT-(Br)COOH. Through the calibration curve of each modifier, we can calculate the amount of each modifier on the TiO_2 nanorods and the results are summarized in Table 1. Through molecular modelling, we have determine that the size of the modifiers is 370.0 Å^3, 87.3 Å^3, 1125.3 Å^3, 2652.6 Å^3 for oleic acid, pyridine, Cu–ph–ether dye, and oligo-3HT-(Br)COOH, respectively (see ESI†). As expected from the molecular size of the modifiers, the amount of pyridine is the highest, the Cu–ph–ether dye is second, and the oligo-3HT-(Br)COOH is the lowest. The amounts of the two modifiers are similar at 4.83×10^{-12} mole cm^{-2} and 2.34×10^{-12} mole cm^{-2} for Cu–ph–ether dye and oligo-3HT-(Br)COOH, respectively. Although the starting concentration of Cu–ph–ether dye is lower than that of oligo-3HT-(Br)COOH, the result clearly indicates the layer formed for the Cu–ph–ether dye on TiO_2 at the beginning cannot be removed by further washing steps.

Table 1 Contact angles of modified TiO_2 with different surface modifiers and adsorbed amount of surface modifiers

Surface Modifier	Contact Angle	Adsorbed Amount (mol cm^{-2})
TiO_2–(pyridine)	95.38° ± 1.06°	2.60×10^{-9} (calculated)
TiO_2–(Cu–ph–ether dye)	106.09° ± 1.28°	4.83×10^{-12}
TiO_2–(oligo-3HT-(Br)COOH)	115.80° ± 1.06°	2.34×10^{-12}

We analyzed the surface chemistry of surface-modified TiO_2 nanorods qualitatively by X-ray photoelectron spectroscopy (XPS). The TiO_2 nanorods were synthesized in oleic acid,[6] so the surfaces of the as-synthesized TiO_2 nanorods contain oleic acid. Fig. 3 shows the results of XPS of TiO_2 before (TiO_2–OA) and after (TiO_2–pyr) pyridine treatment. The oleic acid-capped TiO_2 nanorods have C 1s peaks ranging from 284 to 286 eV, with a normal distribution centred at 285 eV (Fig. 3(a)); Ti $2p_{3/2}$ peak ranges from 458 to 460 eV, with a normal distribution centred at 458.8 eV and the Ti $2p_{1/2}$ peak ranges from 463 to 466 eV, with a normal distribution centred at 464.4 eV (Fig. 3(b)). The position of these peaks is consistent with the literature data.[31,32] The decrease of the C 1s signal with a slight peak shift after pyridine treatment indicates that oleic acid has been replaced by pyridine. Owing to the removal of the larger oleic acid molecules, the electrons from the Ti $2p_{3/2}$ and Ti $2p_{1/2}$ orbitals can easily escape from the sample and are detected more easily (can be realized as the diminishing of the "sheltering effect" of oleic acids), causing the increase in intensity of these two peaks. XPS spectra of the O region were also taken (Fig. 3(c)). Electrons from the O 1s orbital of TiO_2 have lower binding energy, and the corresponding peak ranges from 529 to 532 eV, centred at 530.1 eV. Electrons from the O 1s orbital of the carboxylic group (–COOH) have a higher binding energy and the corresponding peak ranges from 531 to 534 eV, consistent with literature data.[33] The decrease of the O 1s peak from the –COOH group can be interpreted as the removal of the oleic acid containing the carboxylic group. The peak position is slightly shifted, which implies the chemical states of related electrons are different after the pyridine treatment. The increase of the O 1s peak from TiO_2 also originates from the diminishing of the "sheltering effect" of the larger size molecule of oleic acid after the pyridine treatment.

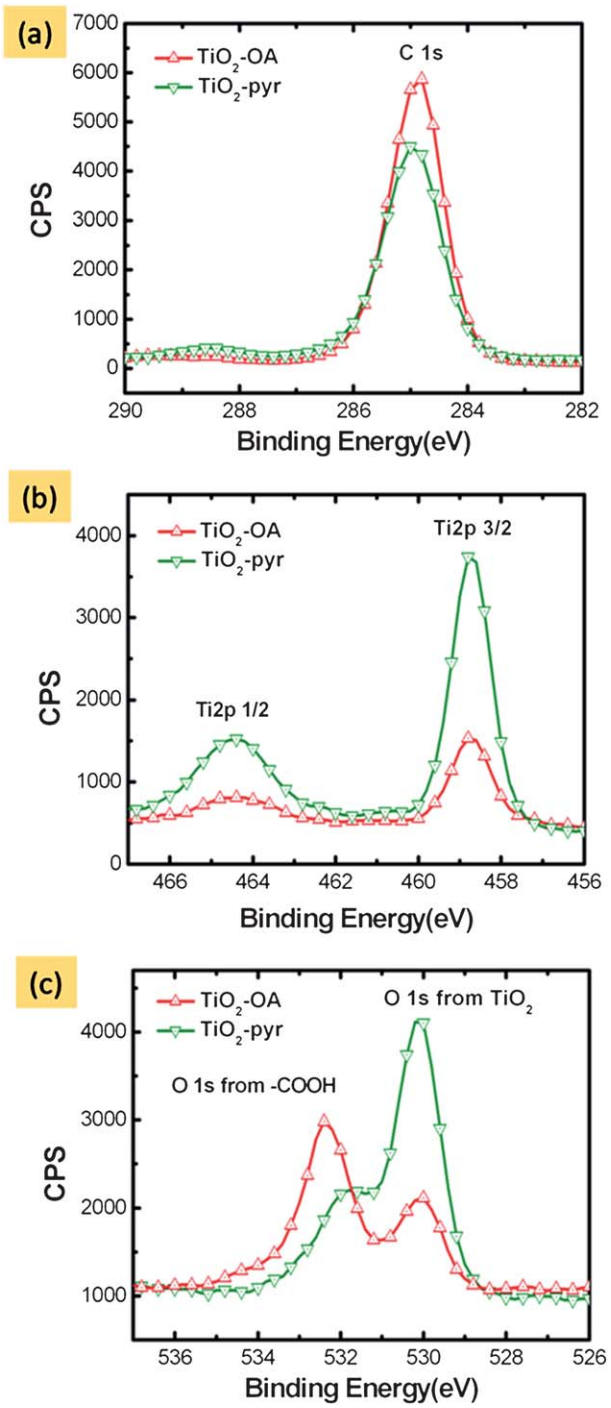

Fig. 3 XPS results of TiO_2 nanorods before (TiO_2–OA) and after (TiO_2–pyr) pyridine treatment for (a) the C 1s orbital, (b) the Ti $2p_{3/2}$ orbital and (c) the O 1s orbital.

Furthermore, when we modified TiO_2 nanorods with oligo-3HT-(Br)COOH and Cu–ph–ether dye; XPS was employed to ensure the adsorption of these interface modifiers. Signals of specific atoms that could only originate from the interface modifier molecules were examined. As shown in Fig. 4(a), TiO_2 nanorods modified with oligo-3HT-(Br)COOH have a S $2p_{3/2}$ peak centred at 168.5 eV, which comes from the sulfur atom of the thiophene ring in oligo-3HT-(Br)COOH. Comparatively, no signal can be observed at the same position for pyridine-treated TiO_2. The adsorption of oligo-3HT-(Br)COOH on TiO_2 is therefore clearly elucidated at the S-atom concentration of 1.40 $\times$ 10^{-10} mole cm^{-2} (Table 1, each molecule contains 60 S-atoms). We were not able to detect the peak of Cu $2p_{3/2}$ (Fig. 4(b)) centred at about 935 eV for Cu–ph–ether dye-modified TiO_2 nanorods, which may be due to the concentration of Cu atoms on the TiO_2 being too low to be detected at 4.83 $\times$ 10^{-12} mole cm^{-2} (Table 1). Nevertheless, the Cu–ph–ether dye is absorbed on the TiO_2 according to its UV-vis spectrum discussed earlier.

We investigated the hydrophobicities of surface-modified TiO_2 by contact angle measurement. The results are summarized in Table 1. To our surprise, the volatile pyridine molecule on the TiO_2 also exhibits hydrophobic behavior. The result indicates that the pyridine is adsorbed on the TiO_2 surface, likely through

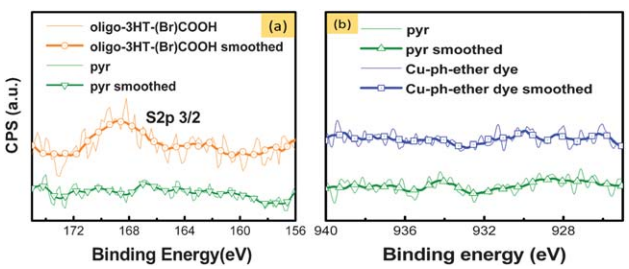

Fig. 4 XPS results of TiO_2 nanorods modified by (a) oligo-3HT-(Br)COOH and (b) Cu–ph–ether dye.

the unshared electron of the nitrogen atom. The hydrophobicity of the surface-modified TiO_2 increases with an increase in the molecular size of the surface modifier in the order oligo-3HT-(Br)COOH ($\theta_{\text{oligo-3HT-(Br)COOH}} = 115.80°$) > Cu–ph–ether dye ($\theta_{\text{Cu–ph–ether dye}} = 106.09°$) > pyridine ($\theta_{\text{pyridine}} = 95.38°$). Thus, a good surface modifier for TiO_2 should be a molecule that contains unshared electrons. The improved surface characteristics of TiO_2 nanorods facilitate the compatibility between TiO_2 and the polymer P3HT.

Fig. 5 displays the TEM images of TiO_2 nanorods modified with the different surface modifiers. Fig. 5(a) shows some aggregations of TiO_2 nanorods modified with pyridine. For surface modification with Cu–ph–ether dye and oligo-3HT-(Br)COOH, the aggregation of TiO_2 nanorods was dramatically reduced (Fig. 5(b) and Fig. 5(c)). The non-aggregated TiO_2 nanorods indicate the nanorods can be well dispersed in P3HT. This result provides large interfacial areas for hybrid systems; consequently, they should provide efficient charge separation and charge transport.

In general, the addition of nanoparticles into the polymer will reduce the flow. Thus, a reduced crystallization of the polymer is observed.[34,35] By modifying the surface of the nanoparticles with organic molecules, compatibility and flow characteristics between organic and inorganic materials are improved. The modifier can function as a plasticizer to help the crystallization of P3HT in the hybrid during the film formation process. We have used synchrotron X-ray spectroscopy to study the changes of P3HT crystallinity by monitoring the diffraction angle 2θ of 5.3° for the primary (100) crystal plane of P3HT. As shown in Fig. 6, the effect of the modifier on the extent of P3HT crystallinity in the hybrid has the order oligo-3HT-(Br)COOH > Cu–ph–ether dye > pyridine. Together with the contact angle and XRD results, we can conclude that the relatively large molecular size of the two new modifiers enhances the compatibility of P3HT and TiO_2; furthermore, they improve the polymer crystallinity in the hybrid films.

We have measured the HOMO and LUMO of P3HT–TiO_2 nanorods with Cu–ph–ether dye and oligo-3HT-(Br)COOH

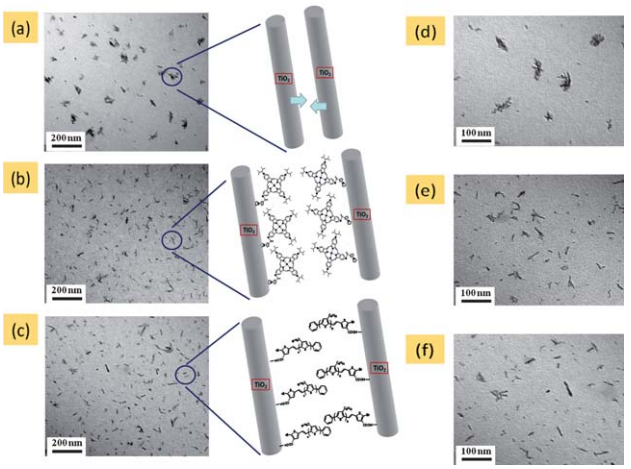

Fig. 5 TEM images of (a) TiO_2–(pyridine), (b) TiO_2–(Cu–ph–ether dye) and (c) TiO_2–(oligo-3HT-(Br)COOH). The corresponding TEM images with higher magnification of (d) TiO_2–(pyridine), (e) TiO_2–(Cu–ph–ether dye) and (f) TiO_2–(oligo-3HT-(Br)COOH) are shown in the right part of the figure.

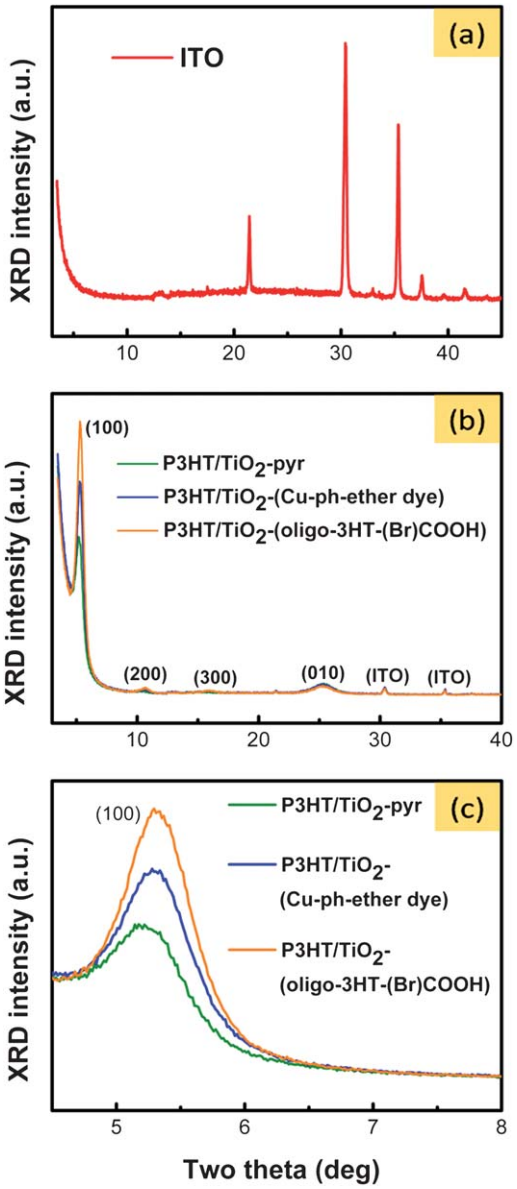

Fig. 6 X-ray diffraction patterns of (a) ITO glass substrate and (b) drop-cast P3HT–TiO_2–(surface modifiers) hybrid films analyzed by synchrotron X-ray spectroscopy. (c) The (100) diffraction peak of P3HT in P3HT–TiO_2–(surface modifiers) hybrid films, the increasing crystallinity is in the order TiO_2 modified with oligo-3HT(Br)-COOH, Cu–ph–ether dye and pyridine.

using cyclic voltammetry. Fig. 7 shows their energy band diagram. The results indicate the two modifiers are well aligned between P3HT and TiO_2 to form a cascade bandgap for enhanced charge transport.

Fig. 8 shows transient photo-voltage data for the hybrid cells fabricated from surface-modified TiO_2 and P3HT. The data was fit into a single-exponential line decay, which falls within the expected range except for a very small voltage perturbation that can be ignored. For P3HT–TiO_2 thin films, the decay of the voltage signal is dependent on the rate of carrier recombination at the P3HT–TiO_2 interface.[36] The charge carrier lifetime can be obtained *via* the exponential fitting line. Thus, we can figure out the recombination rate constant (k_{rec}) from the inverse of the

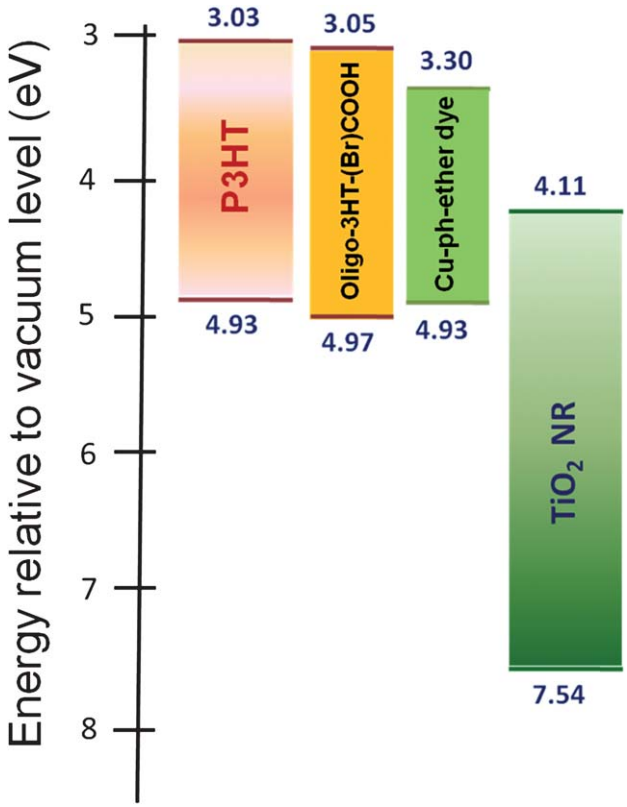

Fig. 7 The band diagram of P3HT–(modifier)–TiO_2.

charge carrier lifetime. Table 2 summarizes the data. These results demonstrate that both modifiers enhance the charge carrier lifetimes and reduce the charge recombination rate constants. Additionally, oligo-3HT-(Br)COOH exhibits a longer lifetime than Cu–ph–ether dye. The oligo-3HT-(Br)-COOH is not as flat as Cu–ph–ether dye and its size is larger (2652.6 Å^3 *vs.* 1125.3 Å^3) so it acts as a more effective energy barrier and spatial obstacle for charge recombination.[8] Moreover, oligo-3HT-(Br)COOH is a conducting material; the polar groups of the carboxylic acid[37] and Br facilitate efficient charge transport to

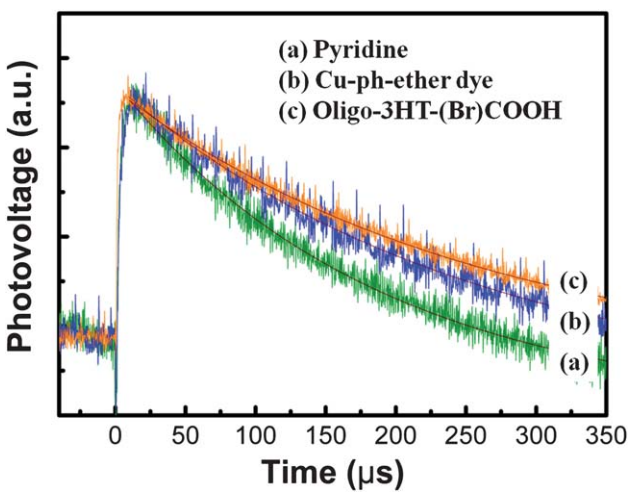

Fig. 8 Photo-voltage transient curves for (a) P3HT–TiO_2–(pyridine), (b) P3HT–TiO_2–(Cu–ph–ether dye) and (c) P3HT–TiO_2–(oligo-3HT-(Br)COOH).

Table 2 Charge carrier lifetime and recombination constant of P3HT–TiO_2–(surface modifier) system

Surface Modifier	Charge Carrier Lifetime, τ (μs)	Recombination Rate Constant, k_{rec} (s^{-1})
TiO_2–(pyridine)	190.2	5.26×10^{-3}
TiO_2–(Cu–ph–ether dye)	259.5	3.85×10^{-3}
TiO_2–(oligo-3HT-(Br)COOH)	300.9	3.32×10^{-3}

reduce charge recombination. The result is consistent with the dipole moment of the modifiers that were calculated by molecular modelling to be 1.5 Debye, 2.4 Debye, 2.6 Debye, 13.7 Debye for oleic acid, pyridine, Cu–ph–ether dye, oligo-3HT-(Br)COOH, respectively (see ESI†).

Fig. 9 illustrates the performance of the modified solar cells under simulated A.M. 1.5 illumination (100 mW cm^{-2}). These results are summarized in Table 3. The increase in open circuit voltage (V_{oc}) after surface modification either by Cu–ph–ether dye or by oligo-3HT-(Br)COOH is attributed to the reduced recombination of charge carriers, which may increase the separation of the *quasi*-Fermi levels.[38] Furthermore, the significant improvement in short circuit current density (J_{sc}) is due to the correlated interfacial behaviors between P3HT and TiO_2 nanorods, which enhance charge separation and charge transport. As expected, the cells fabricated from P3HT–TiO_2–(oligo-3HT-(Br)COOH) outperform P3HT–TiO_2–(Cu–ph–ether dye) and P3HT–TiO_2–pyridine cells.

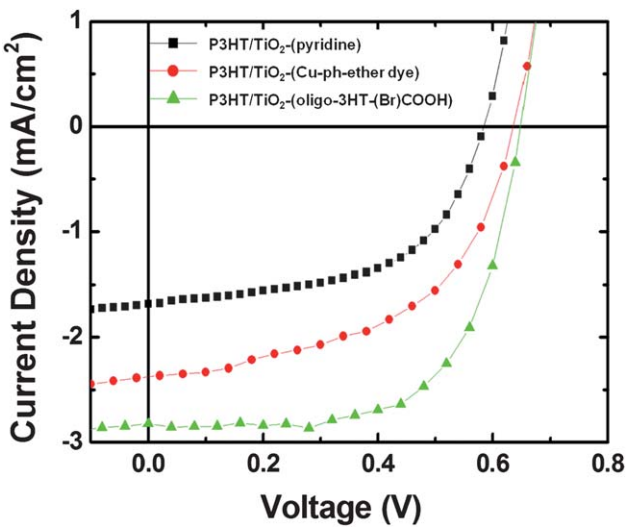

Fig. 9 *J–V* Characteristics of photovoltaic devices based on the P3HT–TiO_2 hybrids using different surface modifiers under A.M. 1.5 illumination (100 mW cm^{-2}).

Table 3 The performance of P3HT–TiO_2 nanorod solar cells using different surface modifiers under A.M. 1.5 illumination (100 mW cm^{-2})

Device	V_{oc} (V)	J_{sc} (mA cm^{-2})	FF	η (%)
P3HT–TiO_2–(pyridine)	0.58	1.68	0.55	0.54
P3HT–TiO_2–(Cu–ph–ether dye)	0.63	2.37	0.52	0.79
P3HT–TiO_2–(oligo-3HT-(Br)COOH)	0.65	2.82	0.64	1.19

Conclusions

The low cost surface modifiers, Cu–ph–ether dye and oligo-3HT-(Br)COOH, are very effective surface modifiers for TiO_2 nanorods. Each modifier makes the TiO_2 nanorods exhibit good hydrophobicity, increasing compatibility with P3HT and allowing for increased dispersion. Most interestingly, these relatively large size modifiers act as plasticizers to increase the crystallinity of P3HT. An efficient charge transport and reduced charge recombination in the hybrid system are observed using these surface-modified TiO_2 nanorods. Consequently, the power conversion efficiency (PCE) of the solar cells has been increased. The oligo-3HT-(Br)COOH modifier shows the largest increase in PCE by 2 times compared with that of the small pyridine molecule. The results point toward a good direction for increasing the efficiency of hybrid solar cells *via* enhancing the interfacial interactions between the organic and inorganic materials.

Acknowledgements

Financial support obtained from the National Science Council of Taiwan (Project No. NSC96-2628-E-002-017-MY3, NSC98-3114-E-002-001 and NSC99-2120-M-002-011) is highly appreciated. We would like to thank Mr. Justin Cochran of the University of California at Santa Barbara for editing the manuscript.

Notes and references

1 W. U. Huynh, J. J. Dittmer and A. P. Alivisators, *Science*, 2002, **295**, 2425–2427.
2 B. Sun, H. J. Snaith, A. S. Dhoot, S. Westenhoff and N. C. Greenham, *J. Appl. Phys.*, 2005, **97**, 014914.
3 S. A. McDonald, G. Konstantatos, S. Zhang, P. W. Cyr, E. J. D. Klem, L. Levina and E. H. Sargent, *Nat. Mater.*, 2005, **4**, 138–142.
4 W. J. E. Beek, M. M. Wienk and R. A. J. Janssen, *Adv. Mater.*, 2004, **16**, 1009–1013.
5 P. Ravirajan, S. A. Haque, J. R. Durrant, D. D. C. Bradley and J. Nelson, *Adv. Funct. Mater.*, 2005, **15**, 609–618.
6 T. W. Zeng, Y. Y. Lin, C. W. Chen, W. F. Su, C. H. Chen, S. C. Liou and H. Y. Huang, *Nanotechnology*, 2006, **17**, 5387–5392.
7 J. Bouclé, S. Chyla, M. S. P. Shaffer, J. R. Durrant, D. D. C. Bradley and J. Nelson, *Adv. Funct. Mater.*, 2008, **16**, 622–633.
8 Y. Y. Lin, T. H. Chu, S. S. Li, C. H. Chuang, C. H. Chang, W. F. Su, C. P. Chang, M. W. Chu and C. W. Chen, *J. Am. Chem. Soc.*, 2009, **131**, 3644–3649.
9 G. Yu, J. Gao, J. C. Hummelen, F. Wudl and A. J. Heeger, *Science*, 1995, **270**, 1789–1791.
10 H. Sirringhaus, N. Tessler and R. H. Friend, *Science*, 1998, **280**, 1741–1744.
11 A. Salleo, T. W. Chen, A. R. Völkel, Y. Wu, P. Liu, B. S. Ong and R. A. Street, *Phys. Rev. B: Condens. Matter Mater. Phys.*, 2004, **70**, 115311.
12 M. Grätzel, *Nature*, 2001, **414**, 338–344.
13 I. S. Liu, H. H. Lo, C. T. Chien, Y. Y. Lin, C. W. Chen, Y. F. Chen, W. F. Su and S. C. Liou, *J. Mater. Chem.*, 2008, **18**, 675–682.
14 C. W. Hsu, L. Y. Wang and W. F. Su, *J. Colloid Interface Sci.*, 2009, **329**, 182–187.
15 J. S. Liu, T. Tanaka, K. Sivula, A. P. Alivisatos and J. M. J. Fréchet, *J. Am. Chem. Soc.*, 2004, **126**, 6550–6551.
16 J. D. Olson, G. P. Gray and S. A. Carter, *Sol. Energy Mater. Sol. Cells*, 2009, **93**, 519–523.
17 J. Kruger, U. Bach and M. Grätzel, *Adv. Mater.*, 2000, **12**, 447–451.
18 N. Kudo, S. Honda, Y. Shimazaki, H. Ohkita, S. Ito and H. Benten, *Appl. Phys. Lett.*, 2007, **90**, 183513.
19 C. Goh, S. R. Scully and M. D. McGehee, *J. Appl. Phys.*, 2007, **101**, 114503.
20 Y. Y. Lin, T. H. Chu, C. W. Chen and W. F. Su, *Appl. Phys. Lett.*, 2008, **92**, 053312.
21 R. Zhu, C. Y. Jiang, B. Liu and S. Ramakrishna, *Adv. Mater.*, 2009, **21**(9), 994.
22 C. W. Tang, *Appl. Phys. Lett.*, 1986, **48**, 183.
23 P. Peumans and S. R. Forrest, *Appl. Phys. Lett.*, 2001, **79**, 126.
24 C. A. Dai, W. C. Yen, Y. H. Lee, C. C. Ho and W. F. Su, *J. Am. Chem. Soc.*, 2007, **129**, 11036–11038.
25 A. S. Amarasekara and M. Pomerantz, *Synthesis*, 2003, 2255–2258.
26 M. J. Frisch, G. W. Trucks, H. B. Schlegel, G. E. Scuseria, M. A. Robb, J. R. Cheeseman, J. A. Montgomery, T. V. Jr., K. N. Kudin, J. C. Burant, J. M. Millam, S. S. Iyengar, J. Tomasi, V. Barone, B. Mennucci, M. Cossi, G. Scalmani, N. Rega, G. A. Petersson, H. Nakatsuji, M. Hada, M. Ehara, K. Toyota, R. Fukuda, J. Hasegawa, M. Ishida, T. Nakajima, Y. Honda, O. Kitao, H. Nakai, M. Klene, X. Li, J. E. Knox, H. P. Hratchian, J. B. Cross, C. Adamo, J. Jaramillo, R. Gomperts, R. E. Stratmann, O. Yazyev, A. J. Austin, R. Cammi, C. Pomelli, J. W. Ochterski, P. Y. Ayala, K. Morokuma, G. A. Voth, P. Salvador, J. J. Dannenberg, V. G. Zakrzewski, S. Dapprich, A. D. Daniels, M. C. Strain, O. Farkas, D. K. Malick, A. D. Rabuck, K. Raghavachari, J. B. Foresman, J. V. Ortiz, Q. Cui, A. G. Baboul, S. Clifford, J. Cioslowski, B. B. Stefanov, G. Liu, A. Liashenko, P. Piskorz, I. Komaromi, R. L. Martin, D. J. Fox, T. Keith, M. A. Al-Laham, C. Y. Peng, A. Nanayakkara, M. Challacombe, P. W. W. Gill, B. Johnson, W. Chen, M. W. Wong, C. Gonzalez and J. A. Pople, *Gaussian 03*, Revision C.02, Gaussian, Inc.: Wallingford CT, 2004.
27 A. D. Becke, *J. Chem. Phys.*, 1993, **98**, 5648–5652.
28 C. T. Lee, W. T. Yang and R. G. Parr, *Phys. Rev. B*, 1988, **37**, 785–789.
29 M. L. Connolly, *J. Appl. Crystallogr.*, 1983, **16**, 548–558.
30 B. Pal, W. C. Yen, J. S. Yang, C. Y. Chao, Y. C. Hung, S. T. Lin, C. H. Chuang, C. W. Chen and W. F. Su, *Macromolecules*, 2008, **41**, 6664–6671.
31 G. Hopfengärtner, D. Borgmann, I. Rademacher, G. Wedler, E. Hums and G. W. Spitznagel, *J. Electron Spectrosc. Relat. Phenom.*, 1993, **63**(2), 91–116.
32 N. Fourches, G. Turban and B. Grolleau, *Appl. Surf. Sci.*, 1993, **68**, 149–160.
33 N. M. D. Brown, J. A. Hewitt and B. J. Meenan, *Surf. Interface Anal.*, 1992, **18**, 187–198.
34 Y. Kim, S. Cook, S. M. Tuladhar, S. A. Choulis, J. Nelson, J. R. Durrant, D. F. C. Bradley, M. Giles, I. Mcculloch, C. S. Ha and M. Ree, *Nat. Mater.*, 2006, **5**, 197–203.
35 L. Nguyen, H. Hoppe, T. Erb, S. Günes, G. Gobsch and N. S. Sariciftci, *Adv. Funct. Mater.*, 2007, **17**, 1071–1078.
36 B. C. O'Regan and F. J. Lenzmann, *J. Phys. Chem. B*, 2004, **108**, 4342–4350.
37 Y. C. Huang, W. C. Yen, Y. C. Liao, Y. C. Yu, C. C. Hsu, M. L. Ho, P. T. Chou and W. F. Su, *Appl. Phys. Lett.*, 2010, **96**, 123501.
38 H. J. Snaith, A. J. Moule, C. Klein, K. Meerholz, R. H. Friend and M. Grätzel, *Nano Lett.*, 2007, **7**, 3372–3376.

